

Pomeranchuk cooling of the $SU(2N)$ ultra-cold fermions in optical lattices

Zi Cai,^{1,2} Hsiang-hsuan Hung,^{1,3} Lei Wang,⁴ Dong Zheng,⁵ and Congjun Wu^{1,6}

¹*Department of Physics, University of California, San Diego, CA92093*

²*Department of Physics and Arnold Sommerfeld Center for Theoretical Physics, Ludwig-Maximilians-Universität München, Theresienstr. 37, 80333 Munich, Germany*

³*Department of Electrical and Computer Engineering, University of Illinois, Urbana-Champaign, Illinois 61801*

⁴*Theoretische Physik, ETH Zurich, 8093 Zurich, Switzerland*

⁵*Department of Physics, Tsinghua University, Beijing, China 100084*

⁶*Key Laboratory of Artificial Micro- and Nano-structures at the Ministry of Education, the School of Physics and Technology at Wuhan University, Wuhan 430072, China*

We investigate the thermodynamic properties of a half-filled $SU(2N)$ Hubbard model in the two-dimensional square lattice by the method of the determinant quantum Monte Carlo simulation, which is free of the fermion “sign problem”. The large number of hyperfine-spin components enhances spin fluctuations, which facilitates the Pomeranchuk cooling to temperatures comparable to the superexchange energy scale in the case of $SU(6)$. Various physical quantities including entropy, charge fluctuations, and spin correlations are calculated.

PACS numbers: 71.10.Fd, 03.75.Ss, 37.10.Jk, 71.27.+a

The $SU(2N)$ and $Sp(2N)$ symmetries are usually studied in high energy physics. They were introduced to condensed matter physics originally as a mathematic convenience. For example, large- N analysis was performed for the $SU(2N)$ symmetric Heisenberg models to systematically handle strong correlation effects [1–4], while realistic electron systems are usually only $SU(2)$ invariant. However, with the recent development of the ultra-cold atom physics, fermion systems with $SU(2N)$ and $Sp(2N)$ symmetries are not just of purely academic interests, but are currently under experimental investigations. It was first pointed out in Ref. [5] that large spin alkali and alkaline-earth fermion systems can exhibit these high symmetries. For example a generic $Sp(4)$, or, isomorphically $SO(5)$ symmetry, can be realized for fermion systems with the hyperfine spin $F = \frac{3}{2}$ without fine-tuning [5, 6]. This $Sp(4)$ symmetry can be further augmented to $SU(4)$ for alkaline-earth fermions, such as ^{135}Ba , ^{137}Ba , and ^{201}Hg because their interactions are hyperfine-spin independent [5]. Experimentally, both the fermionic atoms of ^{173}Yb and ^{87}Sr have been cooled down to quantum degeneracy [7–9]. The ^{173}Yb ($F = I = \frac{5}{2}$) and ^{87}Sr ($F = I = \frac{9}{2}$) systems exhibit the $SU(6)$ and $SU(10)$ symmetries, respectively. Using alkaline-earth fermions to study the $SU(2N)$ symmetry was also proposed in Ref. [10].

The $SU(2N)$ Hubbard model exhibits interesting phenomena that are absent in the standard $SU(2)$ formulation. It is known that quantum spin fluctuations are enhanced by the large number of fermion components [11]. This effect gives rise to exotic quantum magnetism in large-spin ultra-cold fermi systems with high symmetries [12–19]. For example, various $SU(2N)$ valence-bond solid and spin liquid states have been proposed that have not been observed in solid state systems before [15, 20, 21].

In addition, as we will show below, the multi-component nature of the $SU(2N)$ Hubbard model also significantly lowers the charge gap of the Mott-insulating states at the intermediate interaction strengths comparable to the bandwidth.

In this paper, we focus on the temperature regime ($t > T \sim J$), which is of current experimental interest. Here t denotes the hopping integral of the Hubbard model, $J = 4t^2/U$ is the antiferromagnetic exchange energy scale, and U is the onsite repulsion. The thermodynamic properties of the half-filled $SU(2N)$ Hubbard model in the 2D square lattice are studied by determinant quantum Monte-Carlo (DQMC) simulations [22, 23], which is an unbiased, non-perturbative method. It is free of the sign problem at half-filling, thus high numerical precision can be achieved down to low temperatures ($T/t \sim 0.1$). (Recently, the high temperature properties of the $SU(2N)$ Hubbard model has been studied from series expansions, which are only accurate at $T \gg \max(t, U)$ [24].) Special attentions are devoted to the interaction-induced adiabatic coolings. We find that the system can be cooled down to the temperature scale at J from an initial temperature accessible in current experiments. This Pomeranchuk cooling effect, though it is very weak in the $SU(2)$ Hubbard model [25, 26], is enhanced in the $SU(6)$ case.

We consider the following $SU(2N)$ Hubbard model defined in the 2D square lattice at half-filling as

$$H = -t \sum_{\langle i,j \rangle, \alpha} (c_{i\alpha}^\dagger c_{j\alpha} + h.c.) + \frac{U}{2} \sum_i (n_i - N)^2, \quad (1)$$

where α runs over the $2N$ components; $\langle i, j \rangle$ denotes the summation over the nearest neighbors; n_i is the total particle number operator on site i defined as $n_i = \sum_{\alpha=1}^{2N} c_{i\alpha}^\dagger c_{i\alpha}$. The chemical potential μ is set to 0 and

thus does not appear explicitly. Eq. 1 is invariant under the particle-hole transformation in bipartite lattices. Similarly to the case of $SU(2)$, it is easy to prove that the sign problem is also absent for the half-filled $SU(2N)$ Hubbard model of Eq. 1 in bipartite lattices in the DQMC simulations.

Below we will present our DQMC simulations of thermodynamic quantities of the $SU(2N)$ Hubbard model with $2N = 4$ and 6 on a $L \times L$ square lattice with the periodical boundary condition. The second order Suzuki-Trotter decomposition is used. The Trotter steps are taken to be $\Delta\tau = \beta/M$, where $\beta = 1/T$ is the inverse of the temperature T and M ranges from 30 to 150 depending on temperatures. We have checked that the simulation results converge with varying the values of $\Delta\tau$. Instead of using the Hubbard-Stratonovich (HS) transformation in the spin channel [27], we adopt the HS transformation in the charge channel which maintains the $SU(2N)$ symmetry explicitly [28]. This method gives rise to errors on the order of $(\Delta\tau)^4$.

Before presenting numerical results, let us explain qualitatively how the $SU(2N)$ generalization of the Hubbard model makes their charge and magnetic properties different from those of the $SU(2)$ case. When deeply inside the Mott insulating state, magnetic properties at low temperatures are determined by superexchange processes. The number of superexchange processes between a pair of nearest-neighbor sites in the $SU(2N)$ case scales as N^2 . This means that the $SU(2N)$ generalization enhances magnetic quantum fluctuations, and thus weakens, or even completely suppresses the long-range anti-ferromagnetic (AF) correlations. These strong magnetic fluctuations greatly enhance the entropy in the temperature regime ($U > T > J$), which is high enough to suppress short-range AF correlations but not sufficient to unfreeze charge fluctuations.

The charge properties in the Mott insulating state are characterized by the charge gap Δ_c : the energy cost to add a particle or a hole into the system. The half-filling case is a particle-hole symmetric point, and thus a particle or hole excitation each cost the same energy for the grand canonical Hamiltonian Eq. 1. In the atomic limit ($U/t \rightarrow \infty$), the charge gap is $\Delta_c \rightarrow U/2$, which is independent of $2N$. However, for the intermediate interactions comparable with the bandwidth, propagations of the extra particle (hole) in the AF background can significantly lower the charge gap. In Fig. 1 (a), we compare the hopping of an extra hole in the AF background of the half-filled $SU(2)$ and $SU(4)$ Mott insulators. In the $SU(4)$ case, there is more than one way for the hole to hop from one site to another. The mobility of the extra hole is increased and thus, in the $SU(2N)$ Mott insulating state, the charge gap is much lower compared to the $SU(2)$ case. We perform the zero temperature projector QMC to extract the charge gap from the unequal-time single-particle correlation functions (see the supplement

ary material) as shown in Fig. 1 (b), which verifies the above argument. Though the charge gap is a ground state property, it is closely related to the thermodynamic properties and Pomeranchuk cooling in the temperature regime we will study ($J < T < U$). Below we will show that the differences of the magnetic and charge properties between the $SU(2N)$ and $SU(2)$ cases facilitate the Pomeranchuk cooling.

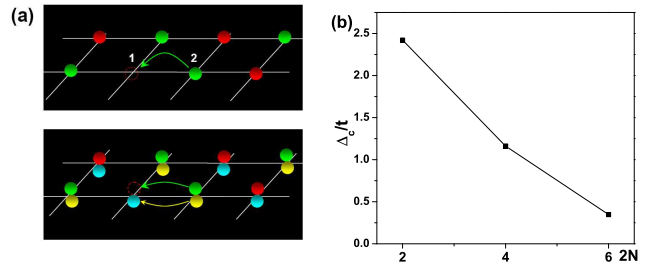


FIG. 1: (a) Sketches of a hole hopping in the $SU(2)$ (up) and $SU(4)$ (down) AF backgrounds, respectively. (b) Charge gaps as a function of $2N$ at $L = 10$ and $U/t = 8$.

Now we address the possibility of cooling down the system by adiabatically increasing interactions. For spinful fermion systems (e.g. ^3He), the Pomeranchuk effect refers to the fact that increasing temperatures can lead to solidification because the entropy (per particle) in the localized solid phase is larger than that of the itinerant Fermi liquid phase. The reason is that, in the Fermi liquid phase, only fermions close to Fermi surfaces within T contribute to entropy. In solids however, each site contributes to nearly $\ln 2 \approx 0.69$ if T is comparable to the spin exchange energy scale of J , which is much smaller than the Fermi energy. In the lattice systems near or at half-filling, increasing interactions suppresses charge fluctuations and drives systems to the Mott-insulating state, thus we would expect Pomeranchuk cooling while adiabatically increasing interactions [29, 30]. However, the situations are complicated by the AF spin correlations which lift the huge spin degeneracy and reduce the entropy in the Mott-insulating state. Actually, for the $SU(2)$ Hubbard model, both at 2D and 3D, DQMC simulations show that the effect of Pomeranchuk cooling is not obvious with interactions up to $U/t \sim 10$ [25, 26, 31].

To investigate the different behaviors between the $SU(2)$ and $SU(2N)$ (-say, $2N = 6$) fermions during the Pomeranchuk cooling, we compare the “entropy capability” (average entropy per atoms) for the half-filled $SU(2)$ and $SU(6)$ Mott insulating states at the same temperature T and U . We focus on the temperature regime ($J < T < U$). For a certain T , the entropy of the Mott insulating state comes from two channels: the spin channel dominated by the spin degeneracy, and the charge channel determined by excitations above the charge gap.

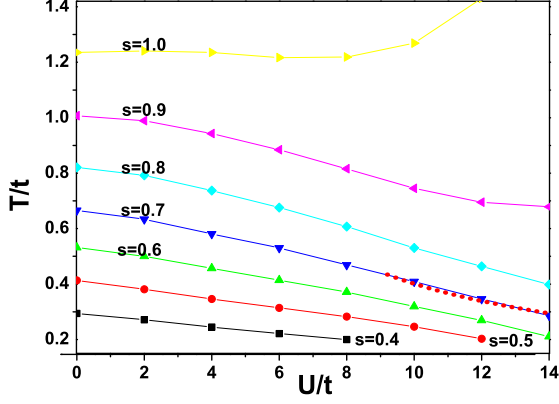


FIG. 2: The isoentropy curves for the half-filled SU(6) Hubbard model on a 10×10 square lattice. The dashed line denotes the spin superexchange scale in strong coupling regime $J/t = 4t/U$.

As we analyzed above, the AF correlations, which lift the spin degeneracy in the SU(2) case, are weakened by the SU($2N$) symmetry. Thus the entropy from the spin contribution in a half-filled SU(6) Mott insulator is larger than that of the SU(2) case. This indicates that the SU(6) Mott insulators have more “entropy capacity” than the SU(2) ones. For example, in the single-atom limit, the spin entropies per atom for SU(2) and SU(6) saturate to the values of $S_{SU(2)} = \ln[C_2^1] = 0.693$ and $S_{SU(6)} = \ln[C_6^3]/3 = 0.998$, respectively, for temperature $T \gg J$. Considering the charge channel will further strengthen this tendency. Since the charge gap of the SU(6) Mott insulating state is smaller than that of the SU(2) case at the same value of U , it is easier to create excitations above the charge gap in the SU(6) case, which further increases entropy. The larger entropic capability of the SU(6) Mott insulating state indicates that it is easier to exhibit the Pomeranchuk effect.

We have confirmed the above picture by performing DQMC simulations. The entropies of the SU(6) Hubbard model are calculated for various parameter values of T and U , and the isoentropy curves are displayed in Fig. 2. The simulated entropy per particle (not per site) is defined as $S_{su(2N)} = S/(NL^2)$, where S is the total entropy in the lattice. It is calculated from the formula

$$\frac{S_{su(2N)}(T)}{k_B} = \ln 4 + \frac{E(T)}{T} - \int_T^\infty dT' \frac{E(T')}{T'^2}, \quad (2)$$

where $\ln 4$ is the entropy at the infinite temperature or, equivalently, $T \gg U$; $E(T)$ denotes the average internal energy per particle at temperature T . For low values of the entropy, adiabatically increasing U leads to a significant cooling to a temperature comparable to the magnetic superexchange scale J , which is an important goal

in current cold atom experiments. This is of direct relevancy to the current experimental progress in ultracold ^{173}Yb atoms [7, 32].

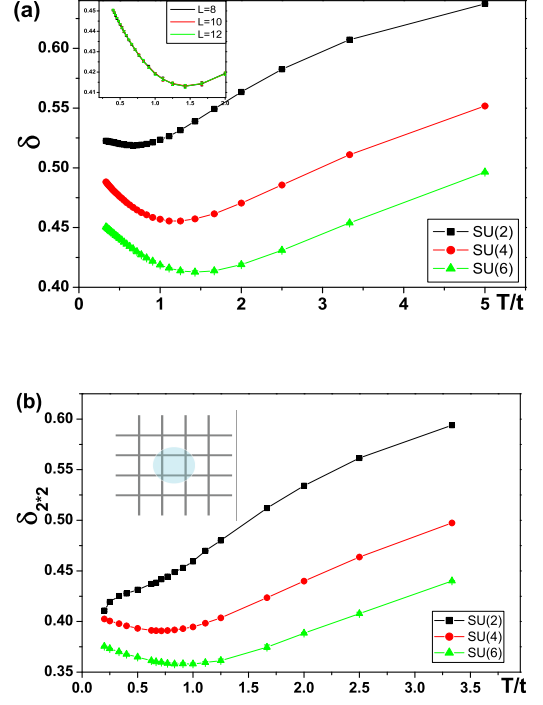


FIG. 3: Particle number fluctuations v.s. T with parameters $U/t = 4$ and different values of $2N$ on a 10×10 lattice. a) The on-site density fluctuations $\delta_{su(2N)}(T)$. The inset shows the convergence of $\delta_{su(6)}(T)$ with $L = 8, 10$, and 12 for the SU(6) case. b) The local particle number fluctuations in a 2×2 sub-volume.

Next we study particle number fluctuations for the half-filled SU($2N$) Hubbard model. The normalized on-site particle fluctuations are defined as

$$\delta_{su(2N)} = \sqrt{\frac{\langle n_i^2 \rangle - \langle n_i \rangle^2}{N}}, \quad (3)$$

where $\langle n_i \rangle = N$. At $T \rightarrow \infty$, $\delta_{su(2N)}$ can be calculated exactly. It is independent of $2N$ as $\delta_{su(2N)}(T \rightarrow \infty) = \frac{\sqrt{2}}{2} \approx 0.71$, which acts as an upper bound on the fluctuations. Similarly, at $U = 0$, $\delta_{su(2N)} = \frac{\sqrt{2}}{2}$ and is independent of both $2N$ and T . For the general case, we plot the DQMC simulation results of δ at a relatively weak interaction strength of $U/t = 4$ over a large range of temperatures seen in Fig. 3 (a). For all the cases, $\delta_{su(2N)}$ is suppressed by U away from the upper limit of $\frac{\sqrt{2}}{2}$. For the cases of SU(4) and SU(6), $\delta_{su(2N)}(T)$ first falls as T increases, which is a reminiscence of the Pomeranchuk effect. Then, after reaching a minimum at T comparable to t , $\delta_{su(2N)}$ grows with increasing T .

This indicates that fermions are localized most strongly at an intermediate temperature scale at which the spin channel contribution to entropy dominates. In comparison, the non-monotonic behavior of $\delta_{su(2N)}$ is weak in the SU(2) case. The above data agrees with the picture that large values of $2N$ enhance spin fluctuations and thus the Pomeranchuk effect. We also calculate the local particle number fluctuations in a small sub-volume: $\delta_{sub} = \sqrt{[\langle \hat{n}_{sub}^2 \rangle - \langle \hat{n}_{sub} \rangle^2] / \langle \hat{n}_{sub} \rangle}$ (\hat{n}_{sub} is the total particle number operator within the sub-volume). As shown in Fig. 3 (b), for the SU(4) and SU(6) cases, the local density fluctuations in a 2×2 sublattice $\delta_{2 \times 2}$ also exhibit non-monotonic behavior similarly to the case of the on-site density fluctuation.

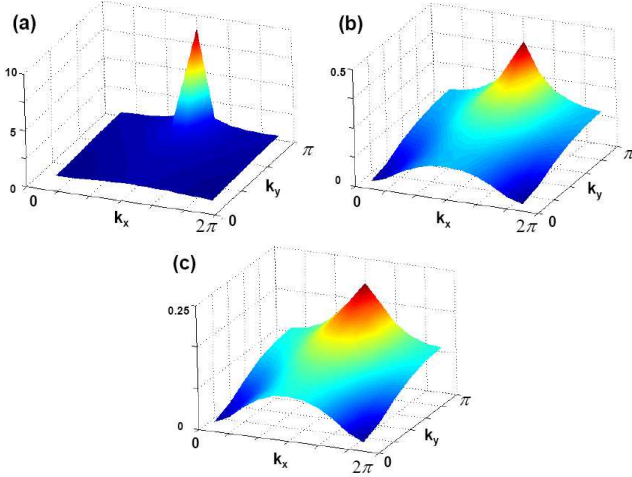


FIG. 4: The normalized spin structure factor $S(\vec{q})$ for the half-filled SU(2N) Hubbard models with $2N$ equal to (a) 2, (b) 4, and (c) 6. Parameter values are $T/t = 0.1$, and $U/t = 8$.

Next we study spin correlations of the SU(2N) Hubbard model. The SU(2N) generators can be represented through fermion operators $c_{i,\alpha}$ ($\alpha = 1 \sim 2N$) as $S_{\alpha\beta,i} = c_{\alpha,i}^\dagger c_{\beta,i} - \frac{1}{2N} \delta_{\alpha\beta} n_i$. There are only $(2N)^2 - 1$ independent operators due to the constraint $\sum_\alpha S_{\alpha\alpha} = 0$. They satisfy the commutation relations $[S_{\alpha\beta,i}, S_{\gamma\delta,j}] = \delta_{i,j} (S_{\alpha\delta,i} \delta_{\gamma\beta} - S_{\gamma\beta,i} \delta_{\alpha\delta})$. We define the SU(2N) version of the two-point equal-time spin-spin correlation as

$$S_{spin}(i, j) = \frac{1}{(2N)^2 - 1} \sum_{\alpha, \beta} \langle S_{\alpha\beta,i} S_{\beta\alpha,j} \rangle. \quad (4)$$

The spin structure factors $S_{su(2N)}(\vec{q})$ are calculated at half-filling and a low temperature, which are defined as

$$S_{su(2N)}(\vec{q}) = \frac{1}{NL^2} \sum_{\vec{i}, \vec{j}} e^{i\vec{q} \cdot \vec{r}} M_{spin}(i, j), \quad (5)$$

where \vec{r} is the relative vector between sites i and j . The distributions of $S_{su(2N)}(\vec{q})$ with $2N = 2, 4, 6$ are plotted in Fig. 4 a), b) and c), respectively. The sharpness of

the peaks at $\vec{q} = (\pi, \pi)$ indicates the dominant AF correlations in all the cases. With increasing $2N$, peaks are broadened showing a weakening of the AF correlations.

The current experimental limit to the entropy per particle for the two-component systems is $S_{su(2)} \sim 0.77k_B$. The corresponding temperature scale is $T \sim t$, which is still larger than J [33]. In contrast, as we analyzed above, the SU(6) Mott insulating state has more “entropy capacity”, which means that for a fixed entropy per atom, the corresponding temperature of the half-filled SU(6) Mott insulating state is lower than that of the SU(2) case. As shown in Fig. 2, for $S_{su(6)} \sim 0.77k_B$, the corresponding temperature of the Mott insulating state ($U/t = 12$) can reach the border of the magnetic superexchange scale J . As for the experimental consequences of the Pomeranchuk cooling, though it is difficult to directly measure temperatures in the lattice, the non-monotonic behavior of the local particle fluctuations, shown in Fig. 3 (a) and (b), can be tested by high-resolution *in situ* measurements which have been used to observe the anti-bunching in ultracold atom Fermi gases [34]. Repeated measurements of the local particle numbers of identically prepared systems give rise to particle fluctuations within the observed volume, which may contain one or several lattice sites. Recently, the Pomeranchuk cooling has been observed in ^{173}Yb fermions in optical lattice (SU(6) Hubbard model). However, we should point an important difference between the experiment and our calculation, namely that the filling factor in the experiment [32] is $1/6$ (one fermion per site) as suppose to the assumed half-filling in our simulations.

In conclusion, we have performed DQMC simulation for the thermodynamic properties of the 2D SU(2N) Hubbard model at half-filling in the temperature regime of direct interest to current experiments. The large numbers of fermion components enhance spin fluctuations, which facilitates the Pomeranchuk cooling to temperatures comparable to the superexchange energy scale. We have focused on half-filling, though it is interesting to ask whether the Pomeranchuk cooling can appear in other filling factors, especially in the case of $1/6$ -filling corresponding to one atom per site in the SU(6) model. In this case, DQMC is plagued by the sign problem. Though in some situations, for example at high temperatures or small values of U , DQMC can still give rise to reliable results if the sign problem is not severe.

We acknowledge J. Hirsch, D. Greif, R. Scalettar and Y. Takahashi for helpful discussions. This work was supported by the NSF DMR-1105945 and the AFOSR FA9550-11-1-0067(YIP) program.

[1] D. P. Arovas and A. Auerbach, Phys. Rev. B **38**, 316 (1988).

- [2] I. Affleck and J. B. Marston, Phys. Rev. B **37**, 3774 (1988).
- [3] N. Read and S. Sachdev, Nucl. Phys. B **316**, 609 (1989).
- [4] N. Read and S. Sachdev, Phys. Rev. Lett. **66**, 1773 (1991).
- [5] C. Wu, J. P. Hu, and S. C. Zhang, Phys. Rev. Lett. **91**, 186402 (2003).
- [6] C. Wu, Mod. Phys. Lett. B **20**, 1707 (2006).
- [7] S. Taie, Y. Takasu, S. Sugawa, R. Yamazaki, T. Tsujimoto, R. Murakami, and Y. Takahashi, Phys. Rev. Lett. **105**, 190401 (2010).
- [8] B. J. DeSalvo, M. Yan, P. G. Mickelson, Y. N. Martinez de Escobar, and T. C. Killian, Phys. Rev. Lett. **105**, 030402 (2010).
- [9] H. Hara, Y. Takasu, Y. Yamaoka, J. M. Doyle, and Y. Takahashi, Phys. Rev. Lett. **106**, 205304 (2011).
- [10] A. V. Gorshkov, M. Hermele, V. Gurarie, C. Xu, P. S. Julienne, J. Ye, P. Zoller, E. Demler, M. D. Lukin, and A. M. Rey, Nature Phys. **6**, 289 (2010).
- [11] C. Wu, Nature Physics **8**, 784785 (2012).
- [12] C. Wu, Phys. Rev. Lett. **95**, 266404 (2005).
- [13] M. A. Cazalilla, A. F. Ho, and M. Ueda, New J. Phys. **11**, 103033 (2009).
- [14] S. R. Manmana, K. R. A. Hazzard, G. Chen, A. E. Feiguin, and A. M. Rey, Phys. Rev. A **84**, 043601 (2011).
- [15] H.-H. Hung, Y. Wang, and C. Wu, Phys. Rev. B **84**, 054406 (2011).
- [16] G. Szirmai, E. Szirmai, A. Zamora, and M. Lewenstein, Phys. Rev. A **84**, 011611 (2011).
- [17] E. Szirmai and M. Lewenstein, Europhys. Lett **84**, 011611 (2011).
- [18] L. S. T. V. M. Colomé-Tatché, C. Klempt, New J. Phys **13**, 113021 (2011).
- [19] F. F. Assaad, Phys. Rev. B **71**, 75103 (2005).
- [20] S. Chen, C. Wu, Y. P. Wang, and S. C. Zhang, Phys. Rev. B **72**, 214428 (2005).
- [21] M. Hermele and V. Gurarie, Phys. Rev. B **84**, 174441 (2011).
- [22] D. J. Scalapino, ArXiv Condensed Matter e-prints (2006), arXiv:cond-mat/0610710.
- [23] J. E. Hirsch, Phys. Rev. B **31**, 4403 (1985).
- [24] K. R. A. Hazzard, V. Gurarie, M. Hermele, and A. M. Rey, ArXiv 1011.0032 (2010), 1011.0032.
- [25] A.-M. Daré, L. Raymond, G. Albinet, and A.-M. S. Tremblay, Phys. Rev. B **76**, 064402 (2007).
- [26] T. Paiva, R. Scalettar, M. Randeria, and N. Trivedi, Phys. Rev. Lett. **104**, 066406 (2010).
- [27] J. E. Hirsch, Phys. Rev. B **28**, 4059 (1983).
- [28] F. F. Assaad, ArXiv Condensed Matter e-prints (1998), arXiv:cond-mat/9806307.
- [29] F. Werner, O. Parcollet, A. Georges, and S. R. Hassan, Phys. Rev. Lett. **95**, 056401 (2005).
- [30] Y. Li, M. R. Bakhtiari, L. He, and W. Hofstetter, Phys. Rev. A **85**, 023624 (2012).
- [31] T. Paiva, Y. L. Loh, M. Randeria, R. T. Scalettar, and N. Trivedi, Phys. Rev. Lett. **107**, 086401 (2011).
- [32] S. Taie, R. Yamazaki, S. Sugawa and Y. Takahashi, Nature Physics **8**, 825 (2012).
- [33] R. Jördens, L. Tarruell, D. Greif, T. Uehlinger, N. Strohmaier, H. Moritz, T. Esslinger, L. De Leo, C. Kollath, A. Georges, et al., Phys. Rev. Lett. **104**, 180401 (2010).
- [34] T. Müller, B. Zimmermann, J. Meineke, J.-P. Brantut, T. Esslinger, and H. Moritz, Phys. Rev. Lett. **105**, 040401 (2010).

Supplementary material

In this supplementary material, we investigate thermodynamic quantities including compressibility and nearest-neighbor spin-spin correlations. These quantities, though not directly related with the Pomeranchuk cooling, are of direct interests in current experiments in ultracold atom physics. They provide a comprehensive understanding of thermodynamical properties of the $SU(2N)$ Hubbard model at half-filling.

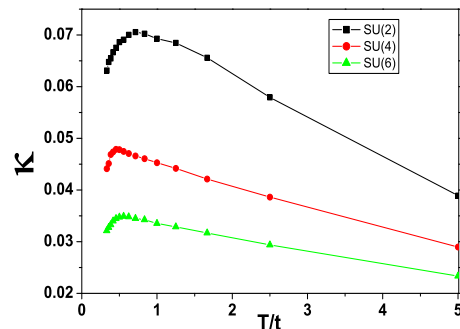


FIG. 5: The normalized compressibility $\kappa_{su(2N)}/(2N)$ v.s. T at $U/t = 4$ for $2N = 2, 4$, and 6 .

Compressibility The compressibility κ can be expressed in terms of the global charge fluctuations as

$$\kappa_{su(2N)} = \frac{1}{L^2} \frac{\partial N_f}{\partial \mu} = \frac{1}{TL^2} (\langle \hat{N}_f^2 \rangle - \langle \hat{N}_f \rangle^2), \quad (6)$$

where $\hat{N}_f = \sum_i \hat{n}_i$ is the total fermion number operator in the lattice; μ is the chemical potential. In Fig. 5, we plot the simulated results for the normalized $\kappa_{su(2N)}/N$, i.e., the contribution to $\kappa_{su(2N)}$ per fermion component. They behave similarly to each other. $\kappa_{su(2N)}$ scales as $1/T$ like ideal gas at high temperatures, while they are suppressed at low temperatures. At zero temperature, $\kappa_{su(2N)}$ is suppressed to zero due to the charge gap in the Mott-insulating states. $\kappa_{su(2N)}$ reaches the maximum at an intermediate temperature scale which can be attributed to the energy scale of charge fluctuations.

Spin susceptibility At finite temperatures, no magnetic long-range-order should exist in the 2D half-filled $SU(2N)$ model due to its continuous symmetry. The normalized uniform $SU(2N)$ spin susceptibility is defined as

$$\chi_{su(2N)}(T) = \frac{\beta}{NL^2} \sum_{\vec{i}, \vec{j}} M_{spin}(\vec{i}, \vec{j}). \quad (7)$$

The DQMC simulation results are presented in Fig. 6 for $U/t = 4$. At high temperatures, $\chi_{su(2N)}$ exhibits the standard Curie-Weiss law which scales proportional to $1/T$. $\chi_{su(2)}$ reaches the maximum at an intermediate temperature at the scale of J below which $\chi_{su(2)}$ is

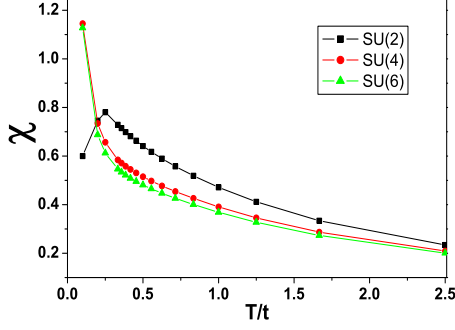


FIG. 6: The normalized $SU(2N)$ susceptibilities $\chi_{su(2N)}$ v.s. T with fixed $U/t = 4$ for $2N = 2, 4$, and 6 .

suppressed by the AF exchange. At the lowest temperature we simulated, we did not observe the suppressions of $\chi_{su(2N)}$ for $2N = 4$ and 6 . The nature of the ground states of half-filled $SU(2N)$ Hubbard model remains an open question in literatures when $2N$ is small but larger than 2 . Nevertheless, we expect that they are either AF long-range-ordered like the case of $SU(2)$, or quantum paramagnetic with or without spin gap like in the large- N limit. In either case, $\chi_{su(2N)}$ should be suppressed to zero with approaching zero temperature.

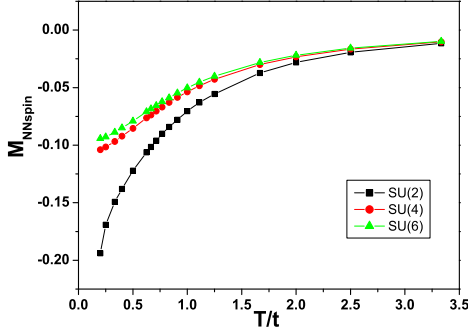


FIG. 7: The normalized NN spin-spin correlation v.s. T/t at $U/t = 4$ for $2N = 2, 4$, and 6 .

The nearest-neighbor spin-spin correlation The nearest-neighbor (NN) spin-spin correlation in the $SU(2N)$ Hubbard model is defined as:

$$M_{spinNN} = \frac{1}{(2N)^2 - 1} \sum_{\alpha, \beta} \langle S_{\alpha\beta, i} S_{\alpha\beta, j} \rangle, \quad (8)$$

where i and j are two nearest-neighbor lattice sites, and $S_{\alpha\beta, i} = c_{\alpha, i}^\dagger c_{\beta, i} - \frac{1}{2N} \delta_{\alpha\beta} n_i$. For the $SU(2)$ Hubbard

model, the NN correlations have been probed recently using the lattice modulation technique [1]. The NN spin-spin correlations v.s. T/t for fixed U/t and different $2N$ have been plotted in Fig. 7. Notice that the monotonic behavior of NN spin-spin correlations as a function of T indicates that these quantities can be used to measure temperatures and entropy in the Mott-insulating states.

Spin-spin correlations in real space In Fig. 8, we plot the renormalized equal time spin-spin correlations for the $SU(2N)$ Hubbard model as a function of distance defined as

$$M_{spin}(r) = \frac{1}{(2N)^2 - 1} \langle \sum_{\alpha, \beta} S_{\alpha\beta}(\mathbf{i}) S_{\beta\alpha}(\mathbf{i} + r\mathbf{e}_x) \rangle, \quad (9)$$

which exhibit a staggered antiferromagnetic structure. For the case of $SU(4)$ and $SU(6)$, spin-spin correlation functions decay much more drastically than that of $SU(2)$. This agrees with the fact that the AF correlations of the $SU(2N)$ Hubbard model are weakened with increasing $2N$.

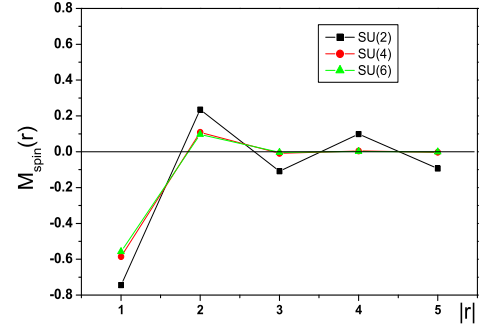


FIG. 8: The normalized spin-spin correlations as functions of distance (along the x -axis) with $T/t = 0.1$, $U/t = 4$ and $2N = 2, 4$, and 6 .

The charge gap The charge gap is defined as the energy cost to add one particle in the ground state of the system composed of N -particles. Assume that

$$\begin{aligned} \hat{H}|\Psi_0^{N+1}\rangle &= E_0^{N+1}|\Psi_n^{N+1}\rangle, \\ \hat{H}|\Psi_0^N\rangle &= E_0^N|\Psi_n^N\rangle, \end{aligned} \quad (10)$$

where \hat{H} is the Hamiltonian of the grand canonical ensemble for the $SU(2N)$ Hubbard model as Eq. (1) in the main text. (The chemical potential μ is set 0 in Eq. (1)). The charge gap is $\Delta_c = E_0^{N+1} - E_0^N$. The onsite time-displaced Green's function for $\tau > 0$ reads

$$G^>(\vec{r}=0, \tau) = \frac{1}{L^2} \sum_i G^>(\tau)_{ii} = \frac{1}{L^2} \sum_i \langle \Psi_0^N | e^{\tau \hat{H}} c_i e^{-\tau \hat{H}} c_i^\dagger | \Psi_0^N \rangle.$$

By inserting the complete set $I = \sum_n |\Psi_n^{N+1}\rangle \langle \Psi_n^{N+1}|$, the above equation becomes

$$G^>(0, \tau) = \frac{1}{L^2} \sum_{i,n} e^{-\tau(E_n^{N+1}-E_0^N)} \langle \Psi_0^N | c_i | \Psi_n^{N+1} \rangle \langle \Psi_n^{N+1} | c_i^\dagger | \Psi_0^N \rangle = \frac{1}{L^2} \sum_{i,n} e^{-\tau(E_n^{N+1}-E_0^N)} |\langle \Psi_0^N | c_i | \Psi_n^{N+1} \rangle|^2. \quad (11)$$

Therefore, at large τ , we have $G^>(\vec{r}=0, \tau) \sim e^{-\tau \Delta_c}$ which can be used to estimate the value of Δ_c [2].

[2] F. F. Assaad and M. Imada, J. Phys. Soc. Jpn **65**, 189 (1996).

[1] D. Greif, L. Tarruell, T. Uehlinger, R. Jördens, and T. Esslinger, Phys. Rev. Lett. **106**, 145302 (2011).